AMERICAN ACADEMY OF OPHTHALMOLOGY®

Genome-wide Meta-analysis for Myopic Macular Neovascularization Identified a Novel Susceptibility Locus and Revealed a Shared Genetic Susceptibility with Age-Related Macular Degeneration

Kazuya Morino, MD,[1,2] Masahiro Miyake, MD, PhD,[1,2] Masao Nagasaki, PhD,[2,3] Takahisa Kawaguchi, PhD,[2] Shogo Numa, MD, PhD,[1,2] Yuki Mori, MD, PhD,[1,2] Shota Yasukura, MD,[1,2] Masahiro Akada, MD,[1,2] Shin-Ya Nakao, MD,[1,2] Ai Nakata, MD,[1,2] Hiroki Hashimoto, BS,[2,3] Ryoko Otokozawa, BAgr,[3] Koju Kamoi, MD, PhD,[4] Hiroyuki Takahashi, MD, PhD,[4] Yasuharu Tabara, PhD,[5] Fumihiko Matsuda, PhD,[2] Kyoko Ohno-Matsui, MD, PhD,[4] Akitaka Tsujikawa, MD, PhD,[1] for the Nagahama Study Group

Purpose: To identify the susceptibility loci for myopic macular neovascularization (mMNV) in patients with high myopia.

Design: A genome-wide association study (GWAS) meta-analysis (meta-GWAS).

Participants: We included 2783 highly myopic individuals, including 608 patients with mMNV and 2175 control participants without mMNV.

Methods: We performed a meta-analysis of 3 independent GWASs conducted according to the genotyping platform (Illumina Asian Screening Array [ASA] data set, Illumina Human610 BeadChip [610K] data set, and whole genome sequencing [WGS] data set), adjusted for age, sex, axial length, and the first to third principal components. We used DeltaSVM to evaluate the binding affinity of transcription factors (TFs) to DNA sequences around the susceptibility of single nucleotide polymorphisms (SNPs). In addition, we evaluated the contribution of previously reported age-related macular degeneration (AMD) susceptibility loci.

Main Outcome Measures: The association between SNPs and mMNV in patients with high myopia.

Results: The meta-GWAS identified rs56257842 at *TEX29 - LINC02337* as a novel susceptibility SNP for mMNV (odds ratio $[OR]_{meta} = 0.62$, $P_{meta} = 4.63 \times 10^{-8}$, $I^2 = 0.00$), which was consistently associated with mMNV in all data sets ($OR_{ASA} = 0.59$, $P_{ASA} = 1.71 \times 10^{-4}$; $OR_{610K} = 0.63$, $P_{610K} = 5.53 \times 10^{-4}$; $OR_{WGS} = 0.66$, $P_{WGS} = 4.38 \times 10^{-2}$). Transcription factor-wide analysis showed that the TFs ZNF740 and EGR1 lost their binding affinity to this locus when rs56257842 had the C allele (alternative allele), and the WNT signaling-related TF ZBTB33 gained binding affinity when rs56257842 had the C allele. When we examined the associations of AMD susceptibility loci, rs12720922 at *CETP* showed a statistically significant association with mMNV ($OR_{meta} = 0.52$, $P_{meta} = 1.55 \times 10^{-5}$), whereas rs61871745 near *ARMS2* showed a marginal association ($OR_{meta} = 1.25$, $P_{meta} = 7.79 \times 10^{-3}$).

Conclusions: Our study identified a novel locus associated with mMNV in high myopia. Subsequent analyses offered important insights into the molecular biology of mMNV, providing the potential therapeutic targets for mMNV. Furthermore, our findings imply shared genetic susceptibility between mMNV and AMD.

Financial Disclosure(s): Proprietary or commercial disclosure may be found in the Footnotes and Disclosures at the end of this article. *Ophthalmology Retina 2025;9:367-377 © 2024 by the American Academy of Ophthalmology. This is an open access article under the CC BY-NC-ND license (http://creativecommons.org/licenses/by-nc-nd/4.0/).*

Supplemental material available at www.ophthalmologyretina.org.

The prevalence of myopia and high myopia is rapidly increasing worldwide and has become a significant public health issue.[1] Myopic macular neovascularization (mMNV) is a major vision-threatening complication of myopia and a leading cause of blindness in developed countries. Similar to other vision-threatening diseases, such as age-related macular degeneration (AMD), macular neovascularization (MNV) plays a central role in the pathogenesis of mMNV.

https://doi.org/10.1016/j.oret.2024.09.016
ISSN 2468-6530/24

Although MNV associated with AMD is primarily triggered by the senescence of the retinal pigment epithelium (RPE) and deposition of drusen, mMNV arises from the rupture of the Bruch's membrane associated with myopia.[2,3] Most MNV can be classified as one of these diseases, with MNV in older individuals predominantly associated with AMD, whereas mMNV accounts for a larger proportion in younger generations.[4] As reported previously, the prognosis of mMNV is poor, with evidence suggesting that, if left untreated, 89% of cases will deteriorate to a visual acuity of 2/20 or worse within 5 years; whereas after 10 years, this figure increases to 96%.[5] This condition is of utmost importance; however, its molecular biologic mechanisms remain largely unknown.

Although the development of MNV associated with AMD is known to be largely driven by genetic factors,[6–8] studies investigating the genetic background of MNV secondary to myopia have been limited. Since the early 2010s, several researchers have conducted candidate gene analyses to explore susceptibility genes for mMNV by evaluating AMD or high myopia susceptibility genes as candidate genes. Although some of these studies identified potential mMNV susceptibility genes, such as *CFI*[9] and *PEDF*,[10] these associations were not well replicated in subsequent studies and thus remain controversial. In addition, no significant association was identified between mMNV development and other candidate genes such as *ARMS2*.[9,11–14] Despite being an era of genome-wide association analysis (GWAS), probably because of the limited sample size compared with AMD, a GWAS for mMNV has not yet been reported. These factors hinder our understanding of mMNV pathogenesis.

In this study, we performed a genome-wide meta-analysis of mMNV to identify well-replicated mMNV susceptibility loci. We also evaluated the association of these loci with previously reported AMD susceptibility genes that showed shared genetic susceptibility between mMNV and AMD.

Methods

Ethics Statement

All human studies were approved by the relevant institutional review boards or medical ethics committees and conducted in accordance with the Declaration of Helsinki. All the participants provided written informed consent.

Participant Enrollment

This study used 2 cohorts: the Kyoto High Myopia Cohort and the Nagahama Study. The Kyoto High Myopia Cohort consisted of highly myopic patients recruited from Kyoto University Hospital, Tokyo Medical and Dental University Hospital, Fukushima Medical University Hospital, Ozaki Eye Hospital, and Kobe City Medical Center General Hospital. The Nagahama Study was a community-based cohort study conducted in Nagahama City, near Kyoto. We used data from baseline visits conducted between 2008 and 2010. We included 3123 individuals with pathologic myopia who had an axial length of at least 25 mm, a spherical equivalent of −5 diopters or lower in at least 1 eye, and were genotyped using either the Human610-Quad BeadChip (Illumina Inc), Illumina HumanHap550 BeadChip, Illumina Human660W-Quad BeadChip, Illumina Infinium Asian Screening Array (ASA)-24 BeadChip, Illumina Infinium Japanese Screening Array-24 BeadChip, or whole genome sequencing (WGS).

We excluded: (1) participants who had macular-involving diseases other than fundus changes due to myopia, such as AMD, retinal vein occlusion, and diabetic retinopathy (203 individuals) and (2) participants who had undergone intraocular surgery (except for cataract surgery) in both eyes (114 participants). If only 1 eye was operated on, information from the nonoperated eye was used. Although the details of the Kyoto High Myopia Cohort and Nagahama Study have been described elsewhere,[10,12,13,15] we briefly summarize them in Supplemental Note (available at www.ophthalmologyretina.org).

Assessment of mMNV

The diagnosis of mMNV was based on clinical findings from slit-lamp biomicroscopy, fluorescein angiography, indocyanine green angiography, spectral-domain OCT, and OCT angiography. Similar to the RADIANCE and MYRROR studies,[16,17] patients were diagnosed with mMNV if MNV was present together with fundus changes compatible with pathologic myopia, namely META-PM category 2–4, and posterior staphyloma. We also included eyes with Fuchs' spot as the mMNV group because Fuchs' spot is known to regress from mMNV and is observed in the scar phase.[18] Patients with MNV secondary to trauma, angioid streaks, uveitis, or any other neovascular maculopathy and those who underwent ocular surgeries other than cataract surgery were excluded. Diagnoses were made by at least 1 retinal specialist.

Creation of 3 GWAS Data Sets According to Genotyping Platform

Three GWAS data sets were created based on the genotyping platform. One is the ASA data set consisting of 1546 individuals genotyped using the Illumina Infinium ASA-24 BeadChip or Illumina Infinium Japanese Screening Array-24 BeadChip. Another is the 610K data set consisting of 772 individuals genotyped using the Illumina Human610-Quad BeadChip, Illumina HumanHap550 BeadChip, or Illumina Human660W-Quad BeadChip. They were grouped together because these DNA microarrays are known to exhibit a largely identical set of measurable single nucleotide polymorphisms (SNPs). The final data set was the WGS data set, consisting of 488 individuals who underwent WGS. These data sets are summarized in Table S1 (available at www.ophthalmologyretina.org). The detailed genotyping and quality control (QC) methods are described in the succeeding sections.

ASA and 610K Data Sets

Genomic DNA was prepared from peripheral blood samples for SNP genotyping, according to standard laboratory procedures. After genome-wide SNP genotyping, stringent initial QC was performed on the participants and SNPs for each data set. Through the QC process, (1) participants with a call rate <0.9; (2) SNPs with a call rate <0.9; (3) SNPs with a minor allele frequency (MAF) <0.01; and (4) SNPs showing deviation from the Hardy-Weinberg equilibrium (HWE; $P < 1.0 \times 10^{-6}$ in control subjects) were excluded. We further excluded participants estimated to have closely related relatives within this population (pi-hat > 0.35).

After the initial QC, genomic imputation was performed for each data set using the Michigan imputation server (https://imputationserver.sph.umich.edu/index.html#!pages/home), with the 1000 Genomes data set (phase3 v5 release) of East Asians as a reference panel for each data set. Then, we conducted secondary

QC; we excluded: (1) imputed SNPs for which R^2 was < 0.6; (2) SNPs with MAF < 0.01; and (3) SNPs showing deviation from the HWE ($P < 1.0 \times 10^{-6}$ in control subjects).

WGS Data Set

For the 274 samples from the Kyoto High Myopia Cohort, DNA from whole blood samples was sequenced on the Illumina HiSeq X using the PCR-free 150 paired-end of 450 base pair fragments protocol. The sequenced raw data were processed, and a FASTQ file was obtained. For these samples, FASTQ was aligned with Burrows-Wheeler Aligner (BWA) version 0.7.17 with the "mem" option to GRCh38DH.fa, and the joint-call operation was conducted with the GATK best practices workflow (GATK ver. 4.1.4).[19] To stabilize the joint-calling accuracy and consistent variant calls to the control data set, we used 11 238 WGS data sets, including the data set from the Nagahama Study, and extracted the variant call format file of eligible samples. From this data set, we selected participants who met the inclusion criteria.

Finally, we applied the same QC as for the other data sets; we excluded: (1) SNPs with a call rate <0.9; (2) SNPs with MAF <0.01; (3) SNPs showing deviation from the HWE ($P < 1.0 \times 10^{-6}$ in control subjects); (4) participants with a call rate < 0.9; and (5) participants estimated to have closely related relatives within this population (pi-hat > 0.35). For the downstream meta-analysis, CrossMap (ver. 0.6.5) was used to modify the GRCh38 coordinates to GRCh37 coordinates to adjust the WGS data set to the same coordinates as the imputed SNP array data sets.[20]

Genome-wide Association Meta-analysis

For the 3 data sets, genome-wide logistic regression analysis was conducted for mMNV, adjusting for age, sex, axial length, and the first to third principal components. PLINK ver. 2.0 (https://www.cog-genomics.org/plink/2.0/) was used for the GWASs. For the genome-wide association meta-analysis (meta-GWAS), we applied the inverse variance-based method and the fixed effects model, as implemented in METAL software (http://www.sph.umich.edu/csg/abecasis/Metal/). Only those SNPs that were present across all 3 data sets and had a heterogeneity I^2 value of less than 0.50 were reported. A P value of $<5.0 \times 10^{-8}$ was considered genome-wide significant. For any genome-wide significantly associated SNP, we evaluated the presence or absence of heterogeneity using I^2 values and forest plots. Unless otherwise specified, R 4.1.0 software (The R Foundation for Statistical Computing) was used for statistical analysis.

Associations of AMD Susceptibility Genes with mMNV

We examined the SNPs of 39 AMD susceptibility loci identified in 3 large AMD GWASs.[6–8] First, we identified the top-hit SNPs for each locus from previous reports (summarized in Table S2, available at www.ophthalmologyretina.org). Second, we determined proxy SNPs (linkage disequilibrium [LD] $r^2 \geq 0.8$ in Japanese in Tokyo) of the top-hit SNPs, so as not to miss the potential signals of the loci. Third, we extracted the SNPs from the meta-analysis results of the 3 GWASs in this study. Finally, we examined whether the extracted SNPs had the same directional effect on MNV development in patients with AMD. The LDpair tool of LDlink (https://ldlink.nih.gov/?tab=home) was used for this analysis.[21] Because we evaluated 39 independent loci, statistical significance was set at a P value $<1.28 \times 10^{-3}$ (0.05/39) for this look-up according to the Bonferroni correction method.

Sensitivity Analysis

Given the large age difference between the cases and controls, we conducted a sensitivity analysis by restricting the control group to individuals aged 60 years or older. For the 3 data sets, logistic regression analysis for mMNV was performed on the SNPs that were genome-wide significant for mMNV or exhibited shared genetic susceptibility between mMNV and AMD, adjusting for age, sex, axial length, and the first to third principal components. Finally, we meta-analyzed these results using METAL with the inverse variance-based method and the fixed effects model.

Associations of mMNV Susceptibility Loci with Axial Length

Because the identified susceptibility loci for mMNV might also be susceptibility loci for axial length, we investigated whether these SNPs were associated with axial length by conducting the mentioned 2 analyses. First, we examined the association between these SNPs and axial length with adjustment for age, sex, and the first to third principal components, using the data from all available participants (N = 8095) with axial length measurements and available genomic DNA samples in the Nagahama Study. The detailed methods for this analysis are described in Supplemental Note (available at www.ophthalmologyretina.org). Second, we searched for previously reported susceptibility SNPs for axial length using the GWAS Catalog, a database maintained by NHGRI that contains summary statistics of all eligible published GWAS studies identified through literature searches and assessed by NHGRI's curators (https://www.ebi.ac.uk/gwas/efotraits/EFO_0005318).

The Impact of SNPs on TF Binding Affinity

DeltaSVM was used to estimate the binding affinity of transcription factors (TFs) to DNA sequences containing SNPs.[22,23] This algorithm relies on an extensive weight database (pretrained weight data) covering all k-mer patterns anchored to a fixed number of bases (e.g., 11 bases) for a TF. This process utilizes large-scale gkm-SVM (LSGKM),[24,25] a machine-learning strategy for predicting TF binding. DeltaSVM contrasts the binding affinity differences in sequences with or without SNPs using pretrained weight data, thereby enabling the prediction of SNP effects on TF interactions. For the pretrained weight data set, we adopted the official weight data set (https://www.beerlab.org/deltasvm_models/) estimated from the 1043 TF binding data sets from the ENCODE2 and ENCODE3 projects.[26] To compare the TF binding affinity difference between the reference and alternative alleles around an SNP, 20 bases upstream and downstream were considered (i.e., 41 bases). For each fixed 11 bases (k-mer), the weights of the reference and alternative k-mer patterns were obtained from the weight database and the difference between them was calculated. The sum of the total differences was used as the delta-score by changing the reference allele to the alternative allele.

Results

Background of the Participants

In total, 2783 participants were included in this study. The backgrounds of the individuals included in the ASA, 610K, and WGS data sets are summarized in Table 3. The ages of the participants in the ASA, 610K, and WGS data sets were 56.74 ± 15.48 years, 51.84 ± 14.99 years, and 56.64 ± 15.67 years, respectively. The axial length of the right/left eyes in the ASA, 610K, and WGS

Table 3. Characteristics of Cases and Controls in This Study

Parameters	ASA			610K			WGS		
	All	*Cases*	*Controls*	*All*	*Cases*	*Controls*	*All*	*Cases*	*Controls*
Number of samples	1527	258	1269	769	241	528	487	109	378
Female	923	202	721	488	185	303	337	73	264
Male	604	56	548	281	56	225	150	36	114
Average age (years)	56.74 ± 15.48	71.27 ± 11.87	53.78 ± 14.43	51.84 ± 14.99	60.34 ± 12.61	47.99 ± 14.42	56.64 ± 15.67	70.68 ± 11.54	52.59 ± 14.32
Axial length (mm)									
OD	26.90 ± 1.63	28.42 ± 1.65	26.59 ± 1.45	28.58 ± 2.51	30.01 ± 1.44	27.92 ± 2.62	28.46 ± 3.18	31.52 ± 1.43	27.59 ± 3.00
OS	26.78 ± 1.61	28.22 ± 1.80	26.49 ± 1.40	28.45 ± 2.47	29.82 ± 1.36	27.82 ± 2.60	28.37 ± 3.22	31.55 ± 1.42	27.46 ± 3.00
Refractive error* (diopters)									
OD	−6.67 ± 4.32	−10.29 ± 7.07	−6.31 ± 3.75	−10.25 ± 6.36	−14.44 ± 8.74	−8.74 ± 6.11	−6.59 ± 5.85	−14.77 ± 9.78	−5.86 ± 4.75
OS	−6.48 ± 4.14	−10.08 ± 6.48	−6.12 ± 3.63	−10.03 ± 6.31	−14.22 ± 8.56	−8.56 ± 6.09	−6.77 ± 5.88	−15.45 ± 9.89	−6.07 ± 4.82

ASA = Asian Screening Array; OD = right eye; OS = left eye; WGS = whole genome sequencing. Data are presented as mean ± standard deviation.
*Refractive error values were obtained only from participants with phakic eyes.
610K, Illumina Human610 BeadChip data set; ASA, Illumina Asian Screening Array data set; WGS, Whole genome sequencing data set.

data sets was 26.90 ± 1.63 mm/26.78 ± 1.61 mm, 28.58 ± 2.51 mm/28.45 ± 2.47 mm, and 28.46 ± 3.18 mm/28.37 ± 3.22 mm, respectively. In all data sets, patients with mMNV were significantly older ($P < 0.01$), predominantly female ($P < 0.01$), and had longer axial lengths ($P < 0.01$).

Meta-GWAS for mMNV in Participants with High Myopia

In total, 3 604 952 SNPs from 608 participants with mMNV and 2175 control participants were meta-analyzed. Figure 1 shows a Manhattan plot of the results of the meta-analysis. The inflation factor (λ_{GC}) was 1.045, with the λ_{GC} of each data set being 1.030, 1.042, and 1.034, for the ASA, 610K, and WGS data sets, respectively, indicating a good control of population sub-structure. Quantile−quantile plots are shown in Figure S2 (available at www.ophthalmologyretina.org).

The results of the meta-analysis are presented in Table 4. The meta-analysis of the 3 data sets revealed that rs56257842 at *TEX29 - LINC02337* was genome-wide significantly associated with mMNV development (odds ratio [OR] [95% confidence interval (CI)] = 0.62 [0.52−0.73], $P = 4.63 \times 10^{-8}$; Table 4). The protective association of rs56257842 C allele at *TEX29 - LINC02337* was consistently observed in all 3 data sets (OR_{ASA} [95% CI] = 0.59 [0.45−0.78], $P_{ASA} = 1.71 \times 10^{-4}$; OR_{610K} [95% CI] = 0.63 [0.48−0.81], $P_{610K} = 5.53 \times 10^{-4}$; OR_{WGS} [95% CI] = 0.66 [0.44−0.99], $P_{WGS} = 4.38 \times 10^{-2}$; Fig 3; Table S5, available at www.ophthalmologyretina.org), with an I^2 value of 0.00. Table S5 (available at www.ophthalmologyretina.org) shows the ASA, 610K, and WGS data set results for the top 3 loci that displayed significant associations with mMNV. Figure 4 shows the regional plot of rs56257842 at *TEX29 - LINC02337* in this meta-analysis.

Associations of AMD Susceptibility Genes with mMNV

Of the 39 AMD susceptibility regions, rs12720922 at *CETP* (OR [95% CI] = 0.52 [0.39−0.70], $P = 1.55 \times 10^{-5}$) was significantly associated with mMNV (Table 6). Figure S5 (available at www.ophthalmologyretina.org) presents the regional association between rs12720922 and *CETP*. The *CETP* rs12720922 A allele corresponds to the *CETP* rs183281136 CA allele, which is a protective allele for AMD, indicating the same directional effect on MNV. Details of the associations between the *CETP* rs12720922 and rs183281136 in Japanese in Tokyo are shown in Figure S6 (available at www.ophthalmologyretina.org). rs61871745 near *ARMS2* (OR [95% CI] = 1.25 [1.06−1.48], $P = 7.79 \times 10^{-3}$), rs181604731 at *CASTOR3P - SPDYE3* near *PILRB* (OR [95% CI] = 2.00 [1.16−3.45], $P = 1.21 \times 10^{-2}$), and rs10760669 at *TGFBR1* (OR [95% CI] = 1.18 [1.01−1.39], $P = 3.94 \times 10^{-2}$) showed nominal association with mMNV, though they were no longer statistically significant after the Bonferroni correction (Table 6). Table S7 (available at www.ophthalmologyretina.org) describes the ASA, 610K, and WGS data set results of the 4 loci that displayed significant associations with mMNV before the Bonferroni correction in this meta-analysis. The comprehensive results are summarized in Table S8 (available at www.ophthalmologyretina.org).

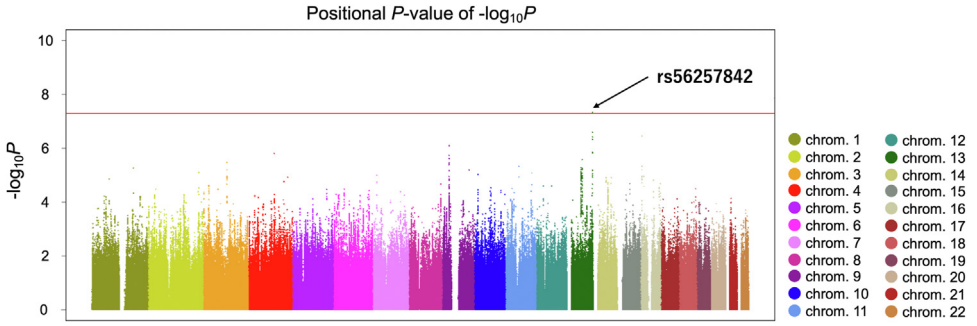

Figure 1. Manhattan plot of the genome-wide meta-analysis for myopic macular neovascularization (mMNV). Each plot shows -$\log_{10}$-transformed *P* values for all SNPs adjusted for age, sex, and axial length. The red horizontal line represents the genome-wide significance threshold ($P = 5.0 \times 10^{-8}$). rs56257842 at *TEX29 - LINC02337* was genome-wide significantly associated with myopic macular neovascularization development (OR [95% CI] = 0.62 [0.52–0.73], $P = 4.63 \times 10^{-8}$).

Sensitivity Analysis

The backgrounds of the participants included in this sensitivity analysis are summarized in Table S9 (available at www.ophthalmologyretina.org). Both rs56257842 at *TEX29 - LINC02337* and rs12720922 at *CETP* demonstrated similar effect sizes between the GWAS and the sensitivity analysis (OR [95% CI] = 0.64 [0.53–0.79], $P = 1.60 \times 10^{-5}$; OR [95% CI] = 0.50 [0.36–0.69], $P = 3.09 \times 10^{-5}$, respectively; Table S10, available at www.ophthalmologyretina.org). Table S10 (available at www.ophthalmologyretina.org) shows the ASA, 610K, and WGS data set results in this sensitivity analysis.

Associations of rs56257842 and rs12720922 with Axial Length

The backgrounds of the participants from the Nagahama Study included in this analysis are summarized in Table S11 (available at www.ophthalmologyretina.org). Neither rs56257842 at *TEX29 - LINC02337* nor rs12720922 at *CETP* showed a significant association with axial length (OR [95% CI] = 0.99 [0.94–1.04], $P = 0.76$; OR [95% CI] = 1.03 [0.96–1.10], $P = 0.46$, respectively; Table S12, available at www.ophthalmologyretina.org). Similarly, neither rs56257842 nor rs12720922 was previously reported as a susceptibility locus for axial length in the GWAS Catalog (Table S13, available at www.ophthalmologyretina.org).

Impact of rs56257842 on the Binding Affinity to TFs

For the 1043 TF binding data from ENCODE Projects 2 and 3, we screened the impact of rs56257842 and calculated the binding affinity and delta-scores for all 1043 TF experiments. Positive binding affinity scores indicated more probable binding. Figure 7A presents a bar plot of the delta-score for TFs ranked within the top 30 for positive and negative delta-scores, respectively. Figure 7B presents a bar plot of the absolute delta-score for those TFs. ZNF740 and EGR1 binding affinity scores of the reference 11mers around rs56257842 (sliding window = 4) exceeded the threshold of positive values, but those of the alternative 11mers did not (Fig 7C, D). Conversely, the ZBTB33 binding affinity score of the alternative 11mers around rs56257842 (sliding window = 4) exceeded the threshold of positive values, whereas that of the reference 11mers did not (Fig 7E). As a result, ZNF740 and EGR1 lost their binding affinity when transitioning from the reference (G) allele to the alternative (C) allele, whereas ZBTB33 gained binding affinity when switching to the alternative (C) allele. ZNF740, ZBTB33, and EGR1 exhibited delta-scores of −13.464, 3.316, and −2.773, respectively. Other TFs of relatively high absolute delta-score, such as MLLT1 and ZNF558, did not change their binding affinity between the reference (G) and alternative (C) alleles, as shown in Figure S8 (available at www.ophthalmologyretina.org). The plots of the top

Table 4. Results of the Meta Genome-wide Analysis for mMNV

SNP	Nearby Gene	CHR	BP	EA/non-EA	Meta-analysis*				
					EAF	*OR (95% CI)*	P	*HetPVal*	I^2
rs1930025	near *LINGO2*	9	27906255	A/G	0.403	0.66 (0.56–0.78)	8.06×10^{-7}	0.90	0
rs56257842	***TEX29 - LINC02337***	**13**	**112166937**	**C/G**	**0.378**	**0.62 (0.52–0.73)**	$\mathbf{4.63 \times 10^{-8}}$	**0.89**	**0**
rs741165	*C16orf89*	16	5105486	A/C	0.380	0.64 (0.54–0.76)	3.50×10^{-7}	0.99	0

The top 3 loci that displayed significant associations with mMNV were extracted. Results of these 3 loci in each data set are summarized in Table S5 (available at www.ophthalmologyretina.org). Boldface indicates the genome-wide significantly associated SNP. The position is based on the National Center for Biotechnology Information build 37.
BP = base pair; CHR = chromosome; CI = confidence interval; EA = effect allele; EAF = effect allele frequency; HetPVal = heterogeneity *P* value between the genome-wide association studies; I^2 = heterogeneity I^2 value between the genome-wide association studies; mMNV = myopic macular neovascularization; non-EA = non-effect allele; OR = odds ratio; SNP = single nucleotide polymorphism.
*Genome-wide association meta-analyses were conducted using the inverse variance method.

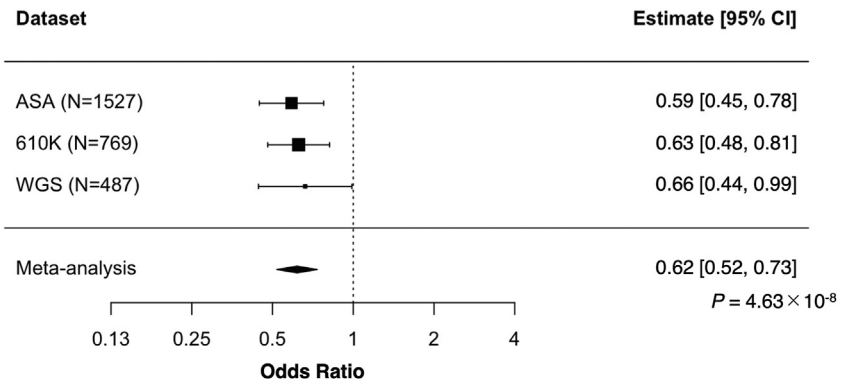

Figure 3. A forest plot depicting the effect of rs56257842 at *TEX29 - LINC02337* on myopic macular neovascularization (mMNV). rs56257842 (effect allele: C) at *TEX29 - LINC02337* showed a consistent effect size on mMNV development in all data sets ($I^2 = 0.00$). The effect size of the single nucleotide polymorphism in each data set was 0.59 (95% confidence interval [CI], 0.45–0.78; $P = 1.71 \times 10^{-4}$), 0.63 (95% CI, 0.48–0.81; $P = 5.53 \times 10^{-4}$), and 0.66 (95% CI, 0.44–0.99; $P = 4.38 \times 10^{-2}$) for the Asian Screening Array (ASA) data set, 610K data set, and whole genome sequencing (WGS) data set, respectively.

8 TFs in absolute binding score are shown in Figure S8 (available at www.ophthalmologyretina.org), and Table S14 (available at www.ophthalmologyretina.org) shows the delta-scores for all 1043 TF experiments.

Discussion

In the current study, we identified rs56257842 at *TEX29 - LINC02337* as a novel susceptibility SNP for mMNV via a meta-GWAS of 608 cases and 2175 controls. Further analysis revealed that the degree of binding of 3 TFs, EGR1, ZNF740, and ZBTB33, to this region was altered by this SNP genotype, suggesting their potential involvement in mMNV development. All of these 3 TFs were expressed in the multiple human retinal cells (Fig S9, available at www.ophthalmologyretina.org).[27] Furthermore, we identified a shared genetic susceptibility to AMD. This study facilitates the understanding of mMNV and blindness in highly myopic eyes.

Although MNV in AMD is associated with tissue aging,[28] MNV in highly myopic eyes is associated with mechanical damage to Bruch's membrane caused by eyeball elongation.[2,3] Both are the leading causes of blindness in developed countries. However, owing to differences in the age of onset, mMNV is the most common etiology of MNV in relatively younger individuals aged less than 50 years.[4] Because the global prevalence of myopia and high myopia is rapidly increasing not only in East Asia but also in the United States and Western Europe,[1] it is important to clarify the pathogenesis of mMNV. However, to date, only a few candidate gene studies, with insufficient subsequent replication, have been conducted, and there are no reports of hypothesis-free analyses, such as GWASs, leaving the

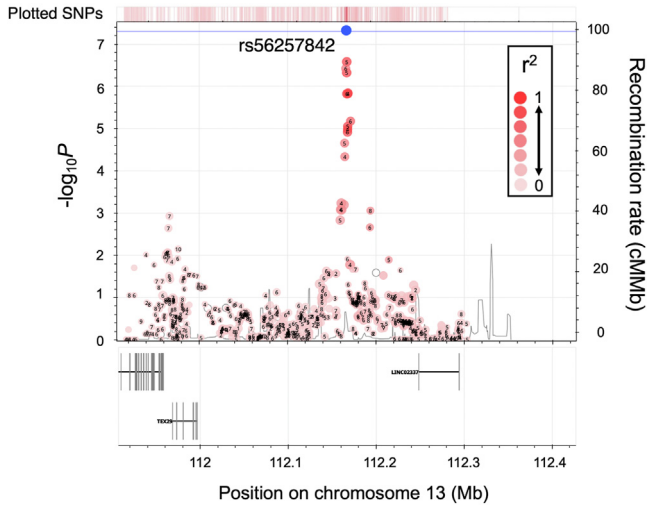

Figure 4. Regional association plots for genotyped single nucleotide polymorphisms (SNPs) around rs56257842 at *TEX29 - LINC02337*. Plots represent the −log10(*P* values) obtained from the genome-wide meta-analysis for SNPs located within 500 000 base pairs of rs56257842. Association signals were observed extending upstream of *LINC02337*.

Table 6. Contribution of AMD Susceptibility Genes on MNV Development in Patients with High Myopia

SNP	Nearby Gene	CHR	BP	R^2	EA/non-EA	Meta-analysis*				
						EAF	*OR (95% CI)*	P	*HetPVal*	I^2
rs181604731	*CASTOR3P - SPDYE3* (near *PILRB*)	7	99894389	0.83	G/A	0.016	2.00 (1.16–3.45)	1.21×10^{-2}	0.98	0
rs10760669	*TGFBR1*	9	101869961	0.89	C/G	0.506	1.18 (1.01–1.39)	3.94×10^{-2}	0.43	0
rs61871745	near *ARMS2*	10	124210369	0.98	A/G	0.389	1.25 (1.06–1.48)	7.79×10^{-3}	0.74	0
rs12720922†	***CETP***	**16**	**57000885**	**1**	**A/G**	**0.100**	**0.52 (0.39–0.70)**	$\mathbf{1.55 \times 10^{-5}}$	**0.39**	**0**

The 4 loci that displayed significant associations with mMNV before the Bonferroni correction were extracted. Results of these 4 loci in each data set are summarized in Table S7 (available at www.ophthalmologyretina.org). Comprehensive results are summarized in Table S8 (available at www.ophthalmologyretina.org). Boldface indicates the significantly associated SNP after the Bonferroni correction. The position is based on the National Center for Biotechnology Information build 37.

AMD = age-related macular degeneration; BP = base pair; CHR = chromosome; CI = confidence interval; EA = effect allele; EAF = effect allele frequency; HetPVal = heterogeneity *P* value between the genome-wide association studies; I^2 = heterogeneity I^2 value between the genome-wide association studies; MNV = macular neovascularization; non-EA = non-effect allele; OR = odds ratio; R^2 = correlation between the lead SNPs from this study and those from AMD studies; SNP = single nucleotide polymorphism.*Genome-wide association meta-analyses were conducted using the inverse variance method.

†A similar result was displayed by rs183281136.

molecular pathogenesis of mMNV largely unknown. Because the association of rs56257842 at *TEX29 - LINC02337* with mMNV reached genome-wide significance in the current meta-GWAS and achieved a statistically significant threshold in each data set, we believe that this SNP is a robust susceptibility SNP for mMNV, which can enhance our understanding of mMNV pathogenesis.

Among the 3 TFs considered to alter the binding affinity in the vicinity of rs56257842 owing to its mutation, EGR1 is the most interesting molecule in the context of angiogenesis and myopia. EGR1 plays a crucial role in the response to vascular endothelial damage and regulates the expression of multiple genes involved in angiogenesis, including *VEGF* and *PDGF*, promoting endothelial cell proliferation, migration, and network formation.[29,30] Furthermore, single-cell analysis of AMD donors identified *EGR1* as an overexpressed gene in choriocapillaris endothelial cells.[31] Intriguingly, EGR1, also known as ZENK, has been most closely associated with the mechanisms underlying the onset of myopia. Studies have shown that EGR1 expression is altered in amacrine cells by the perception of defocus, contributing to the suppression of myopia,[32] and that *Opn5* expression in mouse retinal ganglion cells might upregulate EGR1 by receiving violet light and suppressing myopia.[33,34] Although transcriptional upregulation of *EGR1* may seem contradictory in its potential effects on both myopia suppression and vascular neovascularization, considering that *EGR1* expression is higher in the choriocapillaris, choroidal arteries and veins, and RPE cells than in amacrine or ganglion cells (Fig S10, available at www.ophthalmologyretina.org),[35] the enhanced EGR1 binding observed in individuals with the rs56257842 mutation may exert a predominant influence on vascular neovascularization rather than myopia suppression.

ZBTB33 encodes a transcriptional regulator known as Kaiso, which is involved in the WNT signaling pathway.[36] We previously reported that the WNT signaling pathway is involved in myopia through GWASs of international collaborations, which represents a particularly interesting coincidence. Among the molecules in the WNT signaling pathway, we found that *WNT7B*, *RSPO1*, and *ZNRF3* were associated with axial length[15,37] and *CTNND2* with high myopia.[38] *RSPO1* and *ZNRF3* can influence all of the 3 WNT signaling pathways (i.e., the WNT/beta-catenin pathway [canonical cascade], the planar cell polarity [PCP] pathway, and the WNT/Ca^{2+} pathway),[39,40] whereas *CTNND2* and *ZBTB33*/Kaiso are only involved in the PCP pathway.[36] The PCP pathway regulates the establishment of polarity and organizes the cytoskeleton within the plane of an epithelium, including the RPE.[41] Considering previous reports that changes in RPE cell polarity can alter VEGF secretion in response to inflammatory cytokines,[42] changes in RPE polarity associated with myopia may predispose patients to develop mMNV.

Another TF, ZNF740, encodes a zinc-finger protein containing 3 ZnF_C2H2 domains and is involved in the regulation of gene expression primarily through DNA binding (https://www.proteinatlas.org/ENSG00000139651-ZNF740). Although the role of *ZNF740* in the human eye has not been defined, searching the STRING database, which provides details regarding protein–protein interactions, has shown that *ZNF740* is co-expressed with bromodomain-containing protein (*BRD*)-2 and *BRD3* (Fig S11, available at www.ophthalmologyretina.org).[43] Bromodomain extraterminal (BET) proteins, such as BRD2, BRD3, and BRD4, promote gene transcription related to inflammation,[44] and inhibition of BET bromodomains has been reported to reduce inflammation in human RPE cells.[45] As mMNV in high myopia is associated with increased levels of inflammatory cytokines such as interleukin (IL)-6 and IL-8, inflammation is likely strongly involved in the development of mMNV.[46] Therefore, ZNF740 may be involved in the development of mMNV via inflammatory responses in the RPE or other retinal cells.

In summary, the protective effect of the C allele of rs56257842 against mMNV may result from one or more mechanisms: suppression of angiogenesis due to decreased

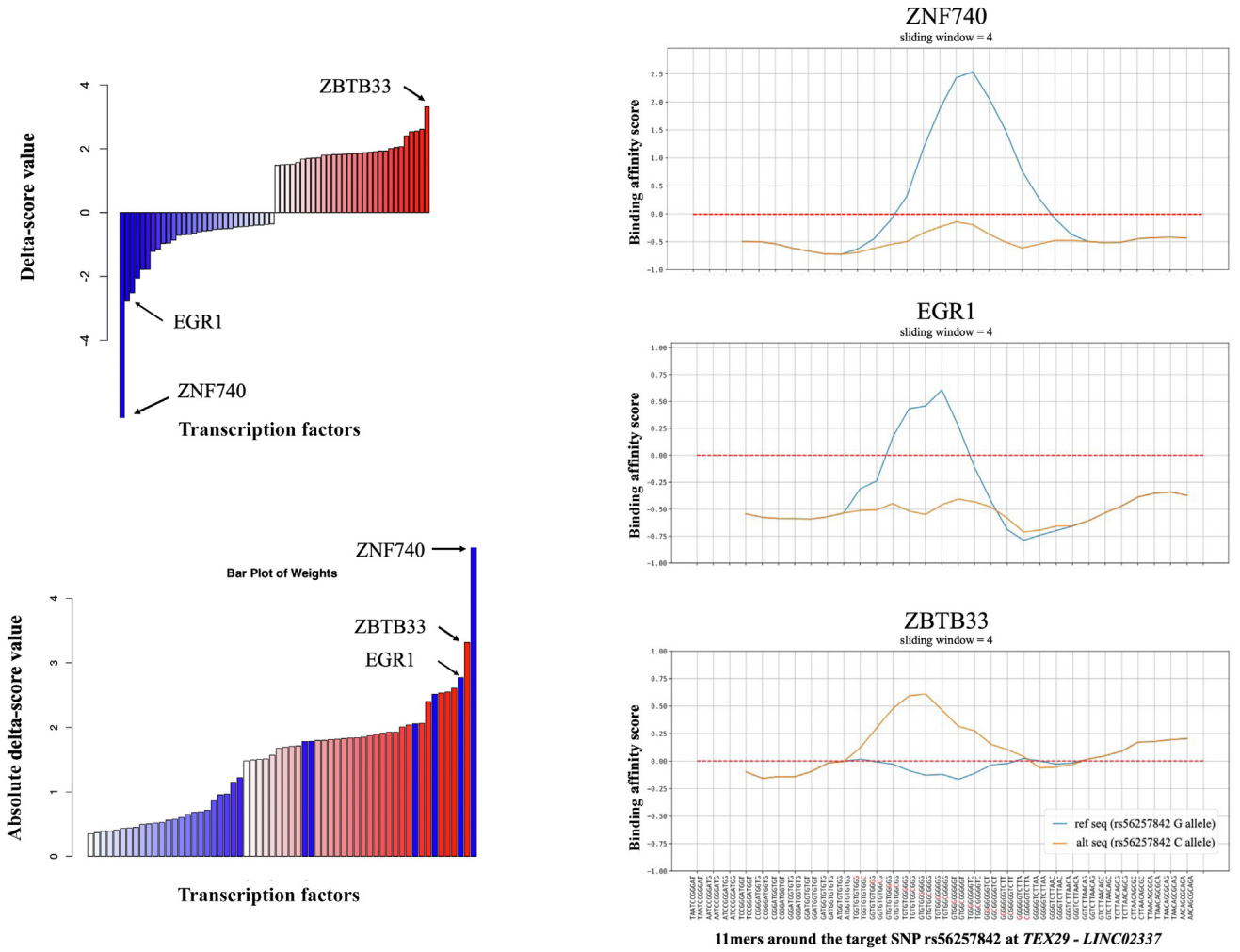

Figure 7. Impact of transcription factor (TF) binding to rs56257842 at *TEX29 - LINC02337*. **A,** Bar plot of delta-scores for TFs that are ranked within the each top 30 for positive and negative delta-scores. TFs with positive delta-scores are presented in red and those with negative delta-scores are presented in blue. **B,** Bar plot of absolute delta-scores for TFs presented in (**A**). The binding affinity score is presented as an absolute value. TFs with positive values are presented in red and those with negative values are in blue. **C**–**E,** Binding affinity scores (vertical axis) of 11mer TF binding motifs around the target SNP rs56257842 at *TEX29 - LINC02337* (horizontal axis) using the machine learning–based prediction method large-scale gkm-SVM; positive scores (above the red dotted lines) indicate more probable binding: **C**, Impact of TF binding for ZNF740 to rs56257842. Around rs56257842 (sliding window = 4), the reference 11mers exceed the threshold of a positive value (red dotted line), whereas alternative 11mers do not. When rs56257842 is G (ref) allele, the maximum binding affinity score is 2.538, but when rs56257842 is C (alt) allele, the maximum binding affinity score is 0. This means that ZNF740 loses the binding affinity when switching to the alternative (**C**) allele. **D,** Impact of TF binding of EGR1 to rs56257842. Around rs56257842 (sliding window = 4), the reference 11mers exceed the threshold of a positive value (red dotted line), whereas alternative 11mers does not. When rs56257842 is G (ref) allele, the maximum binding affinity score is 0.608, but when rs56257842 is C (alt) allele, the maximum binding affinity score is less than 0. This means that EGR1 loses the binding affinity when switching to the alternative (**C**) allele. **E**, Impact of TF binding of ZBTB33 to rs56257842. Around rs56257842 (sliding window = 4), the alternative 11mers exceed the threshold of a positive value (red dotted line), whereas reference 11mers does not. When rs56257842 is C (alt) allele, the maximum binding affinity score is 0.609, but when rs56257842 is G (ref) allele, the maximum binding affinity score is less than 0. This means that ZBTB33 gains the binding affinity when switching to the alternative (**C**) allele.

binding affinity of EGR1; regulation of RPE cell polarity through WNT signaling due to increased binding affinity of ZBTB33; or suppression of inflammatory responses due to decreased binding affinity of ZNF740, either individually or in combination. These mechanisms could serve as potential therapeutic targets for mMNV and thus warrant further molecular biologic investigation. Considering that the change in binding affinity of ZNF740 to rs56257842 was much greater than that of the other TFs, ZNF740 may be a particularly promising therapeutic target for mMNV.

Because mMNV shares its pathology with AMD in terms of MNV, researchers are interested in their genetic correlation. However, though GWASs have been extensively conducted for AMD,[6–8] such analyses for mMNV have not yet been performed, leaving the genetic similarities between these conditions largely unknown. This study provides robust

evidence through a GWAS indicating that mMNV and AMD share a genetic background. *CETP* is associated with AMD in both White and Asian populations,[7,8] and the deterioration of *CETP* function increases the risk of AMD onset and elevates serum high-density lipoprotein cholesterol levels.[47] Although the association between *CETP* rs3764261 and mMNV has been previously investigated in a White cohort without identifying a significant association, this is likely due to underpowering caused by the very small sample size (71 cases and 196 controls).[9] Considering the relatively strong effect (OR [95% CI] = 0.52 [0.39−0.70] for rs12720922 A allele) observed in the current study, further investigation is needed to elucidate how *CETP* is involved in mMNV. Meanwhile, *ARMS2* showed a nominally significant association with mMNV, but considering the multiplicity of testing, the association was not significant. Previous reports also failed to identify a significant association between *ARMS2* and mMNV.[9,11,12] As such, *ARMS2* either does not contribute to the development of mMNV, or if it does, its effect is not substantial.

Although this study uncovered a novel genome-wide significant hit, this study has some limitations. The first limitation is the sample size. Because this study identified only one genome-wide significant novel hit, more samples are needed to elucidate the biomolecular mechanisms of mMNV using GWASs. Another limitation is that although this study confirmed the association with reproducibility across 3 data sets, all of these were from a single Japanese ethnic group. Whether this association is replicated in other ethnic groups requires further investigation. Third, large differences were in the background characteristics between cases and controls. However, we carefully adjusted for possible intermediate variables such as age, sex, and axial length. Additionally, sensitivity analysis did not show any notable changes in effect sizes of rs56257842 at *TEX29* - *LINC02337* and rs12720922 at *CETP*. Considering the fact that these SNPs have not been reported as susceptibility loci for myopia-related traits, we believe that we could identify true signals for mMNV.

In conclusion, we report the results of a genome-wide meta-analysis on mMNV development in patients with high myopia, and the subsequent analyses offer important insights into the molecular biology of mMNV, providing potential therapeutic targets for mMNV. Further genetic studies will reveal the pathogenesis of mMNV in patients with high myopia.

Acknowledgments

The authors thank Ms Hatsue Hamanaka for her assistance with genotyping the Kyoto High Myopia Cohort. They also acknowledge Yuri Aikawa for supporting the partial implementation of the in-house data analysis platform based on LSGKM. The infrastructure of the Omics Science Center Secure Information Analysis System, Medical Institute of Bioregulation at Kyushu University, provided (part of) the computational resources. This work was supported in part by the MEXT Cooperative Research Project Program, Medical Research Center Initiative for High Depth Omics, and CURE:JPMXP1323015486 for MIB, Kyushu University.

Footnotes and Disclosures

Originally received: April 16, 2024.
Final revision: September 26, 2024.
Accepted: September 26, 2024.
Available online: November 1, 2024. Manuscript no. ORET-D-24-00362R2.

[1] Department of Ophthalmology, Kyoto University Graduate School of Medicine, Kyoto, Japan.

[2] Center for Genomic Medicine, Kyoto University Graduate School of Medicine, Kyoto, Japan.

[3] Division of Biomedical Information Analysis, Medical Research Center for High Depth Omics, Medical Institute of Bioregulation, Kyushu University, Fukuoka, Japan.

[4] Department of Ophthalmology and Visual Science, Tokyo Medical and Dental University, Tokyo, Japan.

[5] Graduate School of Public Health, Shizuoka Graduate University of Public Health, Shizuoka, Japan.

Disclosures:

All authors have completed and submitted the ICMJE disclosures form.

K.O.-M.: Consultant − Santen Pharmaceutical, CooperVision Inc.

M.M.: Grants − Novartis Pharma, Daiich-Sankyo, Kaneka Corporation, Rohto Pharmaceutical; Payment or honoraria − Bayer Yakuhin, Novartis Pharma, AMO Japan, Santen Pharmaceutical, Senju Pharmaceutical, Johnson & Johnson K.K., Chugai Pharmaceutical, Japan Ophthalmic Instrument Association, Findex, Topcon Corporation, Sysmex Corporation.

Y.M.: Consultant − Santen Pharmaceutical, Kowa Company.

S.N.: Payment or honoraria − Senju Pharmaceutical, Santen Pharmaceutical, Janssen Pharmaceutical, Kowa Pharmaceutical, Bayer Yakuhin.

A.T.: Grants − Canon, Findex, Santen Pharmaceutical, Sumitomo Pharma, Otsuka Pharmaceutical, Senju Pharmaceutical, Alco Japan, Bayer Yakuhin, Wakamoto Pharmaceutical, Chugai Pharmaceutical, AMO Japan, Rohto Nitten; Consultant − Senju Pharmaceutical, Boehringer Ingelheim, Chugai Pharmaceutical, Bayer Yakuhin, HOYA, Janssen Pharmaceutical, Sumitomo Pharma, Kyowa Kirin, Alcon Japan; Payment or honoraria − Santen Pharmaceutical, Senju Pharmaceutical, Novartis Pharma, Bayer Yakuhin, Chugai Pharmaceutical, Alcon Japan, Otsuka Pharmaceutical, AMO Japan, Wakamoto Pharmaceutical, Kowa Company, MSD, Ellex, HOYA, Canon, Johnson & Johnson K.K., Rohto Pharmaceutical, Nikon Solutions.

Members of the Nagahama Study Group: Takeo Nakayama, MD, PhD, Akihiro Sekine, PhD, Shinji Kosugi, MD, PhD, Yasuharu Tabara, PhD, and Fumihiko Matsuda, PhD.

The other authors have no proprietary or commercial interest in any materials discussed in this article.

Financial Disclosure(s):

Funded by Japan Society for the Promotion of Science (JSPS KAKENHI): JP25293141 (Y.T.), JP26293198 (K.C.), JP26670313 (Y.T.), JP17H04123 (Y.T.), JP17H04126 (K.A.), JP17H04182 (K.C.), JP18K18450 (Y.T.), JP18H02955 (A.T.), JP19K17634 (S.H.), JP21H03092 (A.T.) and JP21H02681 (M.N.). Japan Agency for Medical Research and Development (AMED): JP16dk0207006 (Y.T.), JP16ek0109070 (F.M.), JP17ek0109196 (F.M.), JP17ek0210066 (H.R.), JP18ek0210096 (K.C.), JP18kk0205008 (F.M.), JP18le0110005 (Y.T.), JP19ek0109283 (F.M.), JP19ek0210081 (Y.S.), JP19le0110013 (Y.T.), JP20ek0109492 (M.N.), JP20ek0109485 (M.N.), JP20dk0207027 (K.T.), JP20ek0109348 (F.M.), JP21ek0210116 (K.C.), JP21ek0109548 (M.N.), JP21tm0724602 (Y.S.), JP21wm0425009 (M.N.), JP22dk0110040 (Y.T.), JP22ek0210146 (Y.S.), JP22tm0424222 (M.N.), JP22tm0724604 (Y.S.), JP23ek0109675 (M.N.), JP23ek0109672 (M.N.), and JP23ek0210194 (M.N.). JST NBDC Grant Number: JPMJND2302 (M.N.). "Joint Usage/Research Center for

Interdisciplinary Large-scale Information Infrastructures" and "High Performance Computing Infrastructure" in Japan: jh200047-NWH (M.N.), jh210018-NWH (M.N.), and jh220014 (M.N.), and jh230016 (M.N.). Takeda Medical Research Foundation (F.M.). Mitsubishi Foundation (Y.T.). Daiwa Securities Health Foundation (Y.T.). Sumitomo Foundation (Y.T.). The sponsor or funding organization had no role in the design or conduct of this research.

HUMAN SUBJECTS: Human subjects were included in this study. All human studies were approved by the relevant institutional review boards and/or medical ethics committees and conducted in accordance with the Declaration of Helsinki. All the participants provided written informed consent.

No animals were used in this study.

Author Contributions:

Conception and design: Miyake

Data collection: Morino, Miyake, Nagasaki, Kawaguchi, Numa, Mori, Yasukura, Akada, Nakao, Nakata, Kamoi, Takahashi, Tabara, Matsuda

Analysis and interpretation: Morino, Miyake, Nagasaki, Mori, Hashimoto, Otokozawa, Tabara, Matsuda, Ohno-Matsui, Tsujikawa

Obtained funding: N/A

Overall responsibility: Morino, Miyake, Nagasaki, Kawaguchi, Numa, Mori, Yasukura, Akada, Nakao, Nakata, Hashimoto, Otokozawa, Kamoi, Takahashi, Tabara, Matsuda, Ohno-Matsui, Tsujikawa

Abbreviations and Acronyms:
AMD = age-related macular degeneration; ***ARMS2*** = age-related maculopathy susceptibility 2; **ASA** = Asian Screening Array; **BET** = bromodomain and extraterminal; ***BRD2*** = bromodomain-containing protein 2; ***BRD3*** = bromodomain-containing protein 3; ***BRD4*** = bromodomain-containing protein 4; **BWA** = Burrows-Wheeler Aligner; ***CASTOR3P*** = CASTOR family member 3 pseudogene; ***CETP*** = cholesteryl ester transfer protein; ***CFI*** = complement factor I; **CI** = confidential interval; ***CTNND2*** = catenin delta 2; **EA** = effect allele; **EAF** = effect allele frequency; ***EGR1*** = early growth response protein 1; **GWAS** = genome-wide association study; **HWE** = Hardy-Weinburg equilibrium; **IL-6** = interleukin-6; **IL-8** = interleukin-8; **LD** = linkage disequilibrium; ***LINC02337*** = long intergenic non-protein coding RNA 2337; **LSGKM** = large-scale gkm-SVM; **meta-GWAS** = genome-wide association meta-analysis; ***MLLT1*** = MLLT1 super elongation complex subunit; **mMNV** = myopic macular neovascularization; **MNV** = macular neovascularization; **OR** = odds ratio; **PCP** = planar cell polarity; ***PDGF*** = platelet-derived growth factor; ***PEDF*** = pigment epithelium−derived factor; ***PILRB*** = paired immunoglobin-like type 2 receptor beta; ***PRDM10*** = PR/SET Domain 10; **QC** = quality control; **RPE** = retinal pigment epithelium; ***RSPO1*** = R-Spondin 1; **SD-OCT** = spectral-domain OCT; **SE** = standard error; **SNP** = single nucleotide polymorphism; ***SPDYE3*** = speedy/RINGO cell cycle regulator family member E3; ***TEX29*** = testis expressed 29; **TF** = transcription factor; **WGS** = whole genome sequencing; ***WNT7B*** = Wnt Family Member 7B; ***ZBTB33*** = zinc-finger and BTB domain containing 33; ***ZNF558*** = zinc-finger protein 558; ***ZNF740*** = zinc-finger protein 740; ***ZNRF3*** = zinc/RING-finger protein 3.

Keywords:
Genetics, Genome-wide association study, Myopic macular neovascularization.

Correspondence:
Masahiro Miyake, MD, PhD, Department of Ophthalmology and Visual Sciences, Kyoto University Graduate School of Medicine, 54 Shogoin-kawahara, Sakyo, Kyoto 606-8507, Japan. E-mail: miyakem@kuhp.kyoto-u.ac.jp.

References

1. Holden BA, Fricke TR, Wilson DA, et al. Global prevalence of myopia and high myopia and temporal trends from 2000 through 2050. *Ophthalmology*. 2016;123:1036−1042.
2. Ohno-Matsui K, Morishima N, Ito M, Tokoro T. Indocyanine green angiographic findings of lacquer cracks in pathologic myopia. *Jpn J Ophthalmol*. 1998;42:293−299.
3. Wong TY, Ohno-Matsui K, Leveziel N, et al. Myopic choroidal neovascularisation: current concepts and update on clinical management. *Br J Ophthalmol*. 2015;99:289−296.
4. Cohen SY, Laroche A, Leguen Y, et al. Etiology of choroidal neovascularization in young patients. *Ophthalmology*. 1996;103:1241−1244.
5. Yoshida T, Ohno-Matsui K, Yasuzumi K, et al. Myopic choroidal neovascularization: a 10-year follow-up. *Ophthalmology*. 2003;110:1297−1305.
6. Akiyama M, Miyake M, Momozawa Y, et al. Genome-wide association study of age-related macular degeneration reveals 2 new loci implying shared genetic components with central serous chorioretinopathy. *Ophthalmology*. 2023;130:361−372.
7. Fritsche LG, Igl W, Bailey JN, et al. A large genome-wide association study of age-related macular degeneration highlights contributions of rare and common variants. *Nat Genet*. 2016;48:134−143.
8. Cheng CY, Yamashiro K, Chen LJ, et al. New loci and coding variants confer risk for age-related macular degeneration in East Asians. *Nat Commun*. 2015;6:6063.
9. Leveziel N, Yu Y, Reynolds R, et al. Genetic factors for choroidal neovascularization associated with high myopia. *Invest Ophthalmol Vis Sci*. 2012;53:5004−5009.
10. Miyake M, Yamashiro K, Nakanishi H, et al. Evaluation of pigment epithelium-derived factor and complement factor I polymorphisms as a cause of choroidal neovascularization in highly myopic eyes. *Invest Ophthalmol Vis Sci*. 2013;54:4208−4212.
11. Fernandez-Robredo P, Maestre SR, Zarranz-Ventura J, et al. Myopic choroidal neovascularization genetics. *Ophthalmology*. 2008;115:1632−1632.
12. Nakanishi H, Gotoh N, Yamada R, et al. ARMS2/HTRA1 and CFH polymorphisms are not associated with choroidal neovascularization in highly myopic eyes of the elderly Japanese population. *Eye (Lond)*. 2010;24:1078−1084.
13. Akagi-Kurashige Y, Kumagai K, Yamashiro K, et al. Vascular endothelial growth factor gene polymorphisms and choroidal neovascularization in highly myopic eyes. *Invest Ophthalmol Vis Sci*. 2012;53:2349−2353.
14. Hayashi H, Yamashiro K, Nakanishi H, et al. Association of 15q14 and 15q25 with high myopia in Japanese. *Invest Ophthalmol Vis Sci*. 2011;52:4853−4858.
15. Miyake M, Yamashiro K, Tabara Y, et al. Identification of myopia-associated WNT7B polymorphisms provides insights into the mechanism underlying the development of myopia. *Nat Commun*. 2015;6:6689.
16. Wolf S, Balciuniene VJ, Laganovska G, et al. RADIANCE: a randomized controlled study of ranibizumab in patients with choroidal neovascularization secondary to pathologic myopia. *Ophthalmology*. 2014;121:682−692.
17. Ikuno Y, Ohno-Matsui K, Wong TY, et al. Intravitreal aflibercept injection in patients with myopic choroidal neovascularization: the MYRROR study. *Ophthalmology*. 2015;122:1220−1227.

18. Ohno-Matsui K, Ikuno Y, Lai TYY, Cheung CM. Diagnosis and treatment guideline for myopic choroidal neovascularization due to pathologic myopia. *Prog Retin Eye Res*. 2018;63:92−106.
19. Nagasaki M, Sekiya Y, Asakura A, et al. Design and implementation of a hybrid cloud system for large-scale human genomic research. *Hum Genome Var*. 2023;10:6.
20. Zhao H, Sun Z, Wang J, et al. CrossMap: a versatile tool for coordinate conversion between genome assemblies. *Bioinformatics*. 2014;30:1006−1007.
21. Machiela MJ, Chanock SJ. LDlink: a web-based application for exploring population-specific haplotype structure and linking correlated alleles of possible functional variants. *Bioinformatics*. 2015;31:3555−3557.
22. Lee D, Gorkin DU, Baker M, et al. A method to predict the impact of regulatory variants from DNA sequence. *Nat Genet*. 2015;47:955−961.
23. Shigaki D, Adato O, Adhikari AN, et al. Integration of multiple epigenomic marks improves prediction of variant impact in saturation mutagenesis reporter assay. *Hum Mutat*. 2019;40:1280−1291.
24. Ghandi M, Lee D, Mohammad-Noori M, Beer MA. Enhanced regulatory sequence prediction using gapped k-mer features. *PLOS Comput Biol*. 2014;10:e1003711.
25. Lee D. LS-GKM: a new gkm-SVM for large-scale datasets. *Bioinformatics*. 2016;32:2196−2198.
26. ENCODE Project Consortium. An integrated encyclopedia of DNA elements in the human genome. *Nature*. 2012;489:57−74.
27. Karlsson M, Zhang C, Méar L, et al. A single-cell type transcriptomics map of human tissues. *Sci Adv*. 2021;7:eabh2169.
28. Coleman HR, Chan CC, Ferris FL, Chew EY. Age-related macular degeneration. *Lancet*. 2008;372:1835−1845.
29. Punetha M, Chouhan VS, Sonwane A, et al. Early growth response gene mediates in VEGF and FGF signaling as dissected by CRISPR in corpus luteum of water buffalo. *Sci Rep*. 2020;10:6849.
30. Silverman ES, Collins T. Pathways of Egr-1-mediated gene transcription in vascular biology. *Am J Pathol*. 1999;154:665−670.
31. Voigt AP, Mullin NK, Stone EM, et al. Single-cell RNA sequencing in vision research: insights into human retinal health and disease. *Prog Retin Eye Res*. 2021;83:100934.
32. Fischer AJ, McGuire JJ, Schaeffel F, Stell WK. Light- and focus-dependent expression of the transcription factor ZENK in the chick retina. *Nat Neurosci*. 1999;2:706−712.
33. Jiang X, Pardue MT, Mori K, et al. Violet light suppresses lens-induced myopia via neuropsin (OPN5) in mice. *Proc Natl Acad Sci U S A*. 2021;118:1−8.
34. Jeong H, Lee D, Jiang X, et al. Opsin 5 mediates violet light-induced early growth response-1 expression in the mouse retina. *Sci Rep*. 2023;13:17861.
35. Voigt AP, Whitmore SS, Lessing ND, et al. Spectacle: an interactive resource for ocular single-cell RNA sequencing data analysis. *Exp Eye Res*. 2020;200:108204.
36. Kim SW, Park JI, Spring CM, et al. Non-canonical Wnt signals are modulated by the Kaiso transcriptional repressor and p120-catenin. *Nat Cell Biol*. 2004;6:1212−1220.
37. Cheng CY, Schache M, Ikram MK, et al. Nine loci for ocular axial length identified through genome-wide association studies, including shared loci with refractive error. *Am J Hum Genet*. 2013;93:264−277.
38. Li YJ, Goh L, Khor CC, et al. Genome-wide association studies reveal genetic variants in CTNND2 for high myopia in Singapore Chinese. *Ophthalmology*. 2011;118:368−375.
39. Kim KA, Wagle M, Tran K, et al. R-spondin family members regulate the Wnt pathway by a common mechanism. *Mol Biol Cell*. 2008;19:2588−2596.
40. Hao HX, Xie Y, Zhang Y, et al. ZNRF3 promotes Wnt receptor turnover in an R-spondin-sensitive manner. *Nature*. 2012;485:195−200.
41. Wang C, Qu K, Wang J, et al. Biomechanical regulation of planar cell polarity in endothelial cells. *Biochim Biophys Acta Mol Basis Dis*. 2022;1868:166495.
42. Terasaki H, Kase S, Shirasawa M, et al. TNF-α decreases VEGF secretion in highly polarized RPE cells but increases it in non-polarized RPE cells related to crosstalk between JNK and NF-κB pathways. *PLOS ONE*. 2013;8:e69994.
43. Szklarczyk D, Kirsch R, Koutrouli M, et al. The STRING database in 2023: protein-protein association networks and functional enrichment analyses for any sequenced genome of interest. *Nucleic Acids Res*. 2023;51:D638−D646.
44. Wang N, Wu R, Tang D, Kang R. The BET family in immunity and disease. *Signal Transduct Target Ther*. 2021;6:23.
45. Hytti M, Tokarz P, Määttä E, et al. Inhibition of BET bromodomains alleviates inflammation in human RPE cells. *Biochem Pharmacol*. 2016;110:71−79.
46. Cheung CMG, Arnold JJ, Holz FG, et al. Myopic choroidal neovascularization: review, guidance, and consensus statement on management. *Ophthalmology*. 2017;124:1690−1711.
47. Nordestgaard LT, Christoffersen M, Lauridsen BK, et al. Long-term benefits and harms associated with genetic cholesteryl ester transfer protein deficiency in the general population. *JAMA Cardiol*. 2022;7:55−64.